Solution of the Neutron Survival Probability Equation by the Eigenfunction Expansion Technique

Patrick F. O'Rourke, Anil K. Prinja

Department of Nuclear Engineering, University of New Mexico, Albuquerque, NM 87131, USA
patricko@unm.edu, prinja@unm.edu

INTRODUCTION

The fate of individual neutron chains plays a defining role in the evolution of the neutron population in a strongly stochastic system, which is defined as a supercritical multiplying medium containing a weak, spontaneous fission source. Weak sources lead to well separated neutron chains in which some chains are short lived while others propagate for unusually long times, leading to large fluctuations in the neutron population. Of particular interest are the survival probability, which gives the probability that the neutron chain has not become extinct, and the divergence probability or probability of initiation (POI), which is the probability that the chain will grow without bound. The ability to numerically compute these probabilities, with high accuracy and without introducing overly restrictive physical approximations, is essential in developing an understanding of the behavior of strongly stochastic systems.

The relevant equations for the probabilities of interest have been given by Bell [1] and consist of nonlinear adjoint transport equations, with the order of the nonlinearity determined by the multiplicity of the fission neutron emission. Bell and Lee [3] subsequently showed that the discrete ordinates method combined with a scaled iteration of the nonlinear terms provided an efficient method for solving the equation for the divergence probability. Much later, by implementing iteration at every time step, this approach was adapted to also compute the survival probability [4, 2]. In this article we investigate an alternative approach based on expansion of the probabilities in terms of k-eigenfunctions and demonstrate the efficacy of this approach by comparing against the nonlinear acceleration method.

THEORY

We consider one-speed neutron transport in a multiplying medium and introduce $P(\boldsymbol{r}, \boldsymbol{\Omega}, t)$, the probability that a chain of neutrons propagated by a single initial neutron introduced into the system, V, at the point $\boldsymbol{r}$ traveling in the direction $\boldsymbol{\Omega}$ at an earlier time t will have survived up to a final time, t_f. The spatiotemporal neutron chain survival probability, derived from the Bell Equation [1], satisfies the following nonlinear adjoint transport equation, introduced in operator form:

$$\left[-\frac{1}{v}\frac{\partial}{\partial t} + T^\dagger \right] P(\boldsymbol{r}, \boldsymbol{\Omega}, t) = \left[S^\dagger + F^\dagger - N \right] P(\boldsymbol{r}, \boldsymbol{\Omega}', t) \qquad (1)$$

where the operators denote:

$$T^\dagger P(\boldsymbol{r}, \boldsymbol{\Omega}, t) = -\boldsymbol{\Omega} \cdot \boldsymbol{\nabla} P(\boldsymbol{r}, \boldsymbol{\Omega}, t) + \Sigma_t(\boldsymbol{r}) P(\boldsymbol{r}, \boldsymbol{\Omega}, t),$$

$$S^\dagger P(\boldsymbol{r}, \boldsymbol{\Omega}', t) = \int_{4\pi} \frac{\mathrm{d}\Omega'}{4\pi} \Sigma_s(\boldsymbol{r}, \boldsymbol{\Omega} \cdot \boldsymbol{\Omega}') P(\boldsymbol{r}, \boldsymbol{\Omega}', t),$$

$$F^\dagger P(\boldsymbol{r}, \boldsymbol{\Omega}', t) = \overline{\nu}\Sigma_f(\boldsymbol{r}) \int_{4\pi} \frac{\mathrm{d}\Omega'}{4\pi} P(\boldsymbol{r}, \boldsymbol{\Omega}', t),$$

$$NP(\boldsymbol{r}, \boldsymbol{\Omega}', t) = \Sigma_f(\boldsymbol{r}) \sum_{j=2}^{J} \frac{(-1)^j \chi_j(\boldsymbol{r})}{j!} \left[\int_{4\pi} \frac{\mathrm{d}\Omega'}{4\pi} P(\boldsymbol{r}, \boldsymbol{\Omega}', t) \right]^j$$

with the final condition

$$\lim_{t \to t_f} P(\boldsymbol{r}, \boldsymbol{\Omega}, t) = \begin{cases} 1, & \text{for } \boldsymbol{r} \in V, \\ 0, & \text{otherwise.} \end{cases}$$

We enforce homogeneous Dirichlet boundary conditions:

$$P(\boldsymbol{r}_b, \boldsymbol{\Omega}, t) = 0 \ \text{ for } \ \boldsymbol{r}_b \in \partial V, \ \boldsymbol{\Omega} \cdot \boldsymbol{e}_b > 0$$

where $\boldsymbol{r}_b$ is a position on the system surface, ∂V, and $\boldsymbol{e}_b$ is the surface unit normal of the system. We are utilizing standard notation for the nuclear quantities and $\chi_j(\boldsymbol{r})/j!$ is the average number of j-tuplet neutron groups emitted per fission and is a function of the neutron multiplicity distribution inherent to every induced fission event.

Owing to the complexity of Eq. 1, it can not be solved directly in the presented form, even for restrictive assumptions on the multiplicity distribution. In the ensuing sections, we demonstrate the applicability of the eigenfunction expansion method to efficiently solve Eq. 1 numerically.

Solution by Eigenfunction Expansion

In an attempt to solve Eq. 1, we employ the eigenfunction expansion method (EEM) by assuming the survival probability is separable in phase space and time. We expand $P(\boldsymbol{r}, \boldsymbol{\Omega}, \tau)$ into a complete set of eigenfunctions,

$$P(\boldsymbol{r}, \boldsymbol{\Omega}, \tau) = \sum_{m=1}^{\infty} \Theta_m(\tau) \Psi_m^\dagger(\boldsymbol{r}, \boldsymbol{\Omega}), \qquad (2)$$

where $\Psi_m^\dagger(\boldsymbol{r}, \boldsymbol{\Omega})$ represents the m^{th} adjoint eigenfunction and $\Theta_m(\tau)$ is the associated time-dependent coefficient. Here, it is convenient to use a normalized survival time,

$$\tau = \frac{t_f - t}{t_l},$$

as the variable describing how many lifetimes into the past the initiating neutron first appears, where $t_l = 1/v\Sigma_a(\boldsymbol{r}_o)$ is a constant and is evaluated at a single point $\boldsymbol{r}_o$.

Upon insertion of Eq. 2 into Eq. 1, and suppressing variable functionality for clarity, we find

$$\sum_{m=1}^{\infty}\left\{\Psi_m^{\dagger}\Sigma_{ao}\frac{\mathrm{d}\Theta_m}{\mathrm{d}\tau}+\Theta_m\left[T^{\dagger}-S^{\dagger}-F^{\dagger}\right]\Psi_m^{\dagger}\right\}=-N\left(\sum_{m=1}^{\infty}\Theta_m\Psi_m^{\dagger}\right). \tag{3}$$

Noting that the square-bracketed factor on the LHS of Eq. 3 is identical to the steady-state adjoint neutron transport equation (NTE), we may cast this bracketed term into the m^{th} k-eigenvalue equation. We obtain the spectrum of eigenfunctions, $\mathbf{\Psi}^{\dagger}$ and corresponding eigenvalues, $\boldsymbol{\lambda}$, by discretizing the adjoint NTE into N discrete ordinates and I spatial cells, then solving the system of IN equations as a generalized eigenvalue problem. As a matrix equation, the system is represented as

$$\left[\mathbf{T}^{\dagger}-\mathbf{S}^{\dagger}\right]\mathbf{\Psi}^{\dagger}=\mathbf{F}^{\dagger}\mathbf{\Psi}^{\dagger}\boldsymbol{\lambda}, \tag{4}$$

where $[\mathbf{T}^{\dagger}-\mathbf{S}^{\dagger}]$ and $\mathbf{F}^{\dagger}$ are IN square matrices, $\boldsymbol{\lambda}$ is a diagonal matrix of generalized eigenvalues and $\mathbf{\Psi}^{\dagger}$ is a full matrix whose columns are the corresponding right eigenvectors. We obtain the eigenspectrum by solving Eq. 4, and the m^{th} k-eigenvalue is determined by reciprocating the (m,m) position of $\boldsymbol{\lambda}$ as $k_m=1/\boldsymbol{\lambda}(m,m)$.

Once Eq. 4, and the forward counterpart, have been solved, we apply the definition of the adjoint operator and the fact that the set of adjoint and forward eigenfunctions are bi-orthogonal, i.e., $\langle\Psi_m, F^{\dagger}\Psi_{m'}^{\dagger}\rangle=\langle\Psi_m^{\dagger}, F\Psi_{m'}\rangle=\gamma_m\delta_{m,m'}$, where γ_m is a normalization coefficient to be determined, and δ is the Kronecker delta.

To exploit this identity, we apply $F^{\dagger}$ onto Eq. 3, multiply by the known forward eigenfunctions $\Psi_{m'}$, and integrate over V and $\mathbf{\Omega}$, to obtain a set of coupled nonlinear ODEs for the time-coefficients:

$$\begin{aligned}\gamma_m\Sigma_{ao}\frac{\mathrm{d}\Theta_m}{\mathrm{d}\tau}&=\sum_{m'=1}^{M}\Theta_{m'}\left[1-\frac{1}{k_{m'}}\right]\int_V\mathrm{d}\boldsymbol{r}[\overline{\nu}\Sigma_f]^2\Phi_m\Phi_{m'}^{\dagger}\\&-\sum_{j=2}^{J}\frac{(-1)^j}{j!}\int_V\mathrm{d}\boldsymbol{r}\overline{\nu}[\Sigma_f]^2\chi_j\Phi_m\left[\sum_{m'=1}^{M}\Theta_{m'}\Phi_{m'}^{\dagger}\right]^j\end{aligned} \tag{5}$$

where $\Phi_m^{\dagger}(\boldsymbol{r})=\int_{4\pi}\mathrm{d}\Omega'\Psi_m^{\dagger}(\boldsymbol{r},\mathbf{\Omega}')/4\pi$ is the m^{th} scalar flux eigenfunction and we have truncated Eq. 2 to some order M and the final condition and normalization factor are

$$\Theta_m(0)=\frac{1}{\gamma_m}\int_V\mathrm{d}\boldsymbol{r}\overline{\nu}\Sigma_f\Phi_m(\boldsymbol{r}),\quad \gamma_m=\int_V\mathrm{d}\boldsymbol{r}\overline{\nu}\Sigma_f\Phi_m(\boldsymbol{r})\Phi_m^{\dagger}(\boldsymbol{r}).$$

By solving the system of M nonlinearly coupled ODEs constituting Eq. 5, either numerically or analytically, we may construct an approximate solution to Eq. 1.

RESULTS AND ANALYSIS

The ensuing results maintain S_{16} discrete ordinates using Gauss-Legendre quadrature weighting and the diamond difference equations are used to represent the spatial domain for all systems simulated. We obtain the eigenspectrum by solving Eq. 4 using the QZ algorithm, and the coupled ODEs, Eq. 5, are solved using the fourth-order Runge-Kutta Method, which are readily available functions in MATLAB.

First, we are concerned with the convergence of the eigenvalue spectrum, which is dependent on the refinement of the spatial domain of Eq. 4, from which IN eigenvalues are obtained. Figure 1 shows the relative error of the k-spectrum for a system very near critical and a highly supercritical system, with $k=1.002$ and $k=1.5$, respectively, for which the reference converged spectrum contains 300 cells for either system. If we choose the maximum deviation from the $I=300$ spectrum to be no more than 2%, we may safely use up to 6 modes with 120 cells for any practical range of criticality we may be interested in, which will be the number of cells used in all ensuing simulations.

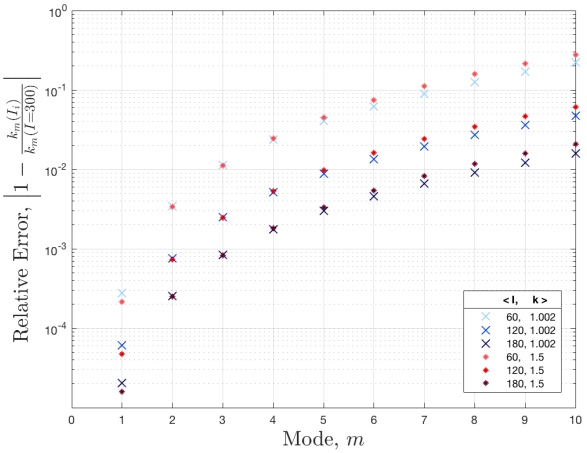

Fig. 1. Relative error of the eigenvalue spectrum for differing I as compared to spectrum values calculated for $I=300$.

As a numerical benchmark for the solutions determined from the EEM, we utilize a well-established nonlinear acceleration method for determining both the POI in static systems [2, 3] as well as the survival probabilities in dynamic systems [4], henceforth referred to as the λ-Acceleration Method (λAM). Solutions to the POI as calculated by the λAM have convergence criteria of 10^{-15} for the fundamental mode (initial guess via the Power Method), the shape of the POI for successive inner iterations, and the convergence of λ onto unity. For probability of survival calculations, time stepping sizes were restricted to widths of $\Delta\tau=0.01$. This acceleration scheme was initially benchmarked against the numerical solution of Eq. 1 obtained by application of Piccard iteration on the nonlinear terms, providing the same results within machine precision.

Figure 2 shows the relative error between the scalar POI as calculated by the EEM relative to the λAM result of the same order of J for a 5.425 cm thick ^{235}U metal slab flanked by graphite slabs, both 2.000 cm thick, in vacuum, for which the fundamental mode is $k=1.15$. The error is largest near the interface, ranging from 0.4% up to 1.1% for the cases shown, due to the more complicated structure of the survival probability, thus the inclusion of higher modes is necessary to capture the neutron chain's response to the abrupt change in

material properties. We see a close coupling of the error for the cases $M = 1, 2$, and a significant drop when 3 modes are used, this could be indicative of an adequate truncation order, although, for this system, even $M = 1$ provides relatively accurate results. Also, note the more accurate representation of the solution near the center for lower modes, this could be due to the 'settling' of the solution into the fundamental mode in areas of the system where the first appearance of the initiating neutron has the highest importance.

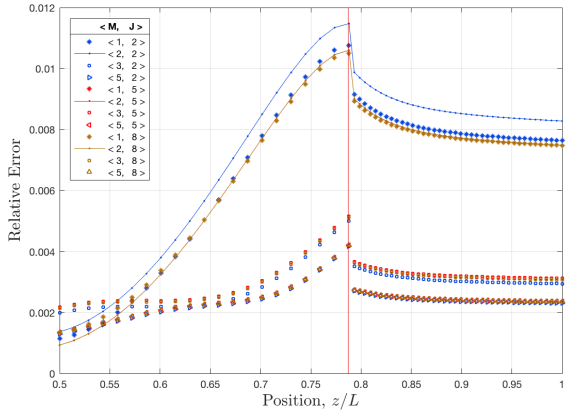

Fig. 2. Relative error of the scalar POI calculated by the EEM as compared to the λAM for differing J, M for a system of $k = 1.15$. The vertical red line designates the $^{235}U - C$ interface.

From the information given by Figure 2, we show in Figure 3, the relative error profile of the scalar POI as calculated by the EEM relative to the λAM solution for the same order J for a near-critical and a highly supercritical system for which the ^{235}U thickness is 4.250 cm and 9.422 cm, respectively. We see the convergence of the error for a slightly supercritical system with $k = 1.002$, the single mode representation agrees for all J with a maximum error occurring at the interface of $\sim 0.5\%$, and similarly for the three mode expansion, but with a scalable difference in the error profile. For the highly supercritical case, we witness the same behavior as before, where the error profiles tend to increase near the center or the slab; it appears necessary to use as many as three modes to reduce the maximum error to around 1%. These plots permit us an insight into the close representation the EEM provides for a select value of J; we now wish to compare any given distribution to an assumed 'true' distribution.

Suppose we take $J = 8$ to be the closest representation of a natural multiplicity distribution of an actual system, we now compare the ascertained distributions for differing M to the 'true' distribution of $J = 8$ obtained from the λAM, depicted in Figure 4. We withhold a comparison with $J = 2$ as the error profiles increase to values above 5% for the $k = 1.15$ and $k = 1.5$ cases; this is expected for such stochastic systems as the inclusion of the full multiplicity distribution will greatly affect the persistence of any given chain. Thus, we retain examples for which the maximum error is around 1%. We see from Figure 4 that for every criticality the $J = 5$ and $J = 8$ provide the same profile for a given M, indicating that we may consider the former, reducing the nonlinearity of the problem with no adverse consequences to the final solution.

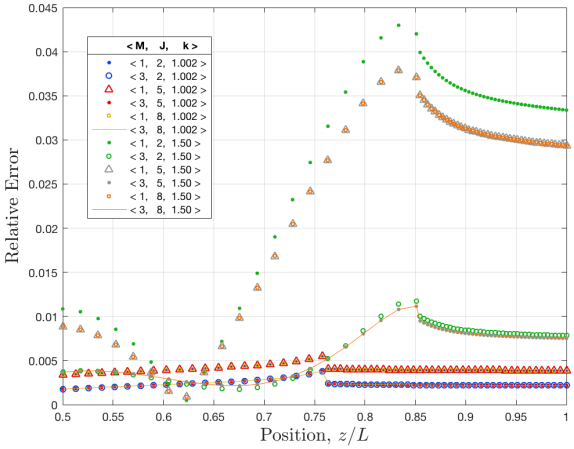

Fig. 3. Relative error of the scalar POI calculated by the EEM as compared to the λAM for a slightly supercritical and a highly critical system for several J and M.

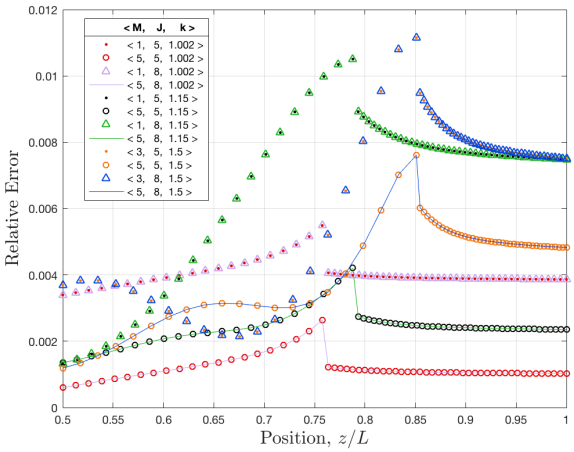

Fig. 4. Relative error as compared to the 'true' distribution.

Figure 5 shows the spatiotemporal profile of the scalar survival probability for the $k = 1.5$ system, previously described. We have truncated the expansion at three modes, $M = 3$, and restricted to a maximum of five neutrons emitted in a fission, $J = 5$. The final condition, $P_o(z, \tau = 0) = 1$, is poorly represented, as expected, since we consider only three of the infinite modes to represent the constant unity profile, but the solution quickly converges within a few lifetimes, indicating that more modes are needed to represent the survival probability for very short times where, again, the EEM tends to fail at approximating constant-in-space profiles. The solution asymptotically approaches the POI as the initial neutron is introduced farther into the past.

Figure 6 shows the POI for the same system described

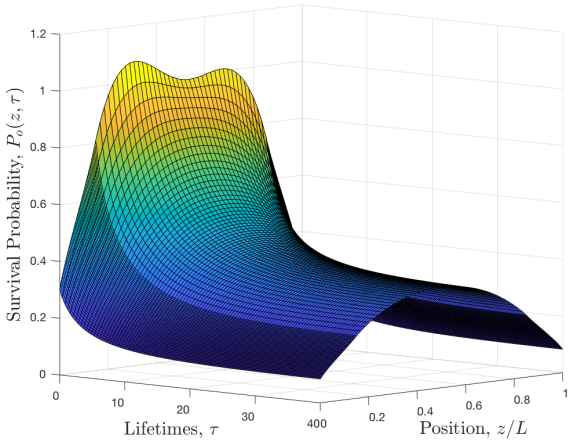

Fig. 5. Convergence of EEM on $P_o(z,\tau)$ and the approach to the POI.

above for several differing orders of nonlinearity attributed to the multiplicity maxima, J, truncation order, M, and fundamental mode, k. In every case, the graphite is 2 *cm* thick, and the inner region thicknesses in *cm* are 5.01, 5.425, and 9.4 for respective k values of 1.002, 1.15, and 1.5. One mode is sufficient for representing the POI, but an appreciable separation arises from the nonlinearity order, where we see $J = 5$ is required for representing the true POI. Figure 7, using the legend of Fig. 6, shows the P_o in the center of the slab for increasing τ, where it is observed that the approach to the POI occurs much faster for higher k systems, as expected, i.e., one may introduce a neutron into the system at times closer to the present to achieve a self-sustaining chain reaction.

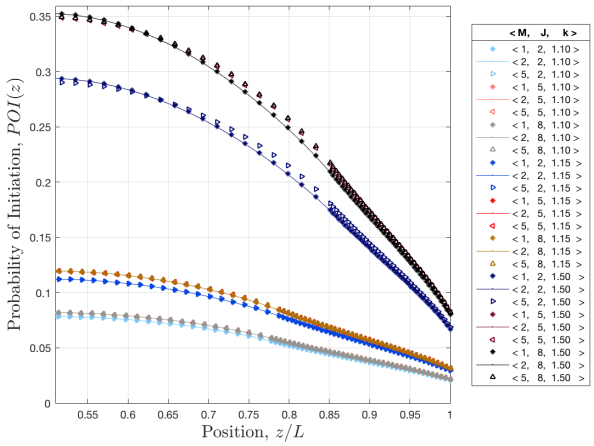

Fig. 6. Spatial distribution of POI for varying multiplicity maxima, J, truncation order, M, and system multiplication, k.

CONCLUSIONS

The eigenfunction expansion method has been employed to construct approximate solutions to neutron chain survival

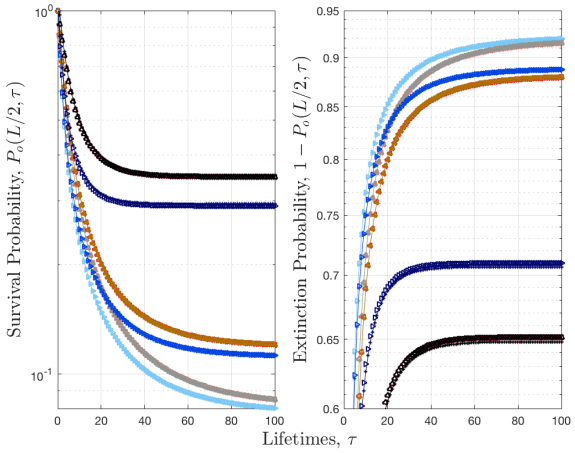

Fig. 7. Demonstration of transition from the probability of survival to the POI after a sufficient number of lifetimes into the past (L) and the complement, the extinction probability (R).

probability equation, where it has been demonstrated to give appreciably the same result as that calculated by a known nonlinear acceleration scheme within several percent. It has been shown that the EEM converges rapidly for low truncation order, represents the solution well for as few as one mode for nearly critical systems and as many as five modes are required for highly multiplying systems. The difference in solutions due to the order of nonlinearity must be taken into account, where order two for near-critical systems, and up to order five for increasing system criticality are necessary.

Forthcoming research entails using the solution to the single-chain survival probability equation to be folded into an equation satisfied by the probability of survival in the presence of a weak neutron source. Also of interest is obtaining the full neutron number probability distribution function, which is not readily available from the current survival probability formulation.

REFERENCES

1. BELL, G., "On the Stochastic Theory of Neutron Transport," Nuclear Science and Engineering, vol. 21, pp. 390-401, 1965.
2. BAKER, R., "Probability of Initiation." Presentation. LA-UR-04-6589. 2005.
3. BELL, G., and LEE, C., " On the Probability of Initiating a Persistent Fission Chain," LA-2608, Los Alamos National Laboratory, 1976.
4. BAKER, R., " Deterministic Methods for Time-Dependent Stochastic Neutron Transport," M & C, 2009.
5. KAMM, R., "Eigenfunction Expansion of the Time and Space-Dependent Neutron Survival Probability Equation." Master's Thesis. University of New Mexico, 2005.